

Development and Analysis of a Novel Nanotherapeutic for the Treatment of Multi-drug Resistant Ovarian Cancer



A Major Qualifying Project Report
Submitted to the Faculty of the
WORCESTER POLYTECHNIC INSTITUTE
in partial fulfillment of the requirements for the
Degree of Bachelor of Science
by:

Jake Brown
Biology and Biotechnology

Libbi Richardson
Biology and Biotechnology

Date: April 2015

Approved:

Professor Mike Buckholt, PhD
Worcester Polytechnic Institute
Biology and Biotechnology

Professor Jill Rulfs, PhD
Worcester Polytechnic Institute
Biology and Biotechnology

Table of Contents

Table of Figures	3
Table of Tables	4
Acknowledgements.....	5
Authorship	6
Abstract	7
Background	8
Introduction	8
Part 1: Ovarian cancer.....	8
Disease Statistics.....	8
Types of Ovarian Cancer	8
Stages.....	10
Existing Treatments	11
Part 2: Cell Death	12
Apoptosis	13
Necrosis.....	13
Autophagy.....	14
Part 3: Emerging, Innovative Cancer Therapies.....	14
Cytotoxics.....	14
Ceramide.....	15
Kinase Inhibitors.....	16
Nanomedicines	17
Folate Targeting	19
Part 4: Hypothesis and Specific Aims.....	21
Materials and Methods.....	22
General Manufacturing Nanomedicines.....	22
HPLC Method of Detecting DTX.....	23
Quantification of APIs in Nanomedicines	23
Cell Lines	23
Cytotoxicity Assay	24
Results.....	27
Manufacturing and Monitoring Stability of Nanomedicines	27
HPLC Detection of DTX.....	29

Cytotoxicity Assays.....	31
Discussion.....	34
References	37

Table of Figures

Figure 1. The stages of ovarian cancer.	10
Figure 2. The types of cell death.....	13
Figure 3. Docetaxel.....	15
Figure 4. Ceramide.....	16
Figure 5. Staurosporine.....	17
Figure 6. Diagram of Generic Nanoparticle. a. Nanoemulsion.....	19
Figure 7. Cytotoxicity Results for DTX, DTX-CER, and DTX-CER-STP nanoemulsions.....	32

Table of Tables

Table 1. The plate layout for cells dose with docetaxel nanoemulsions.	25
Table 2. The plate layout for cells dose with staurosporine and/or combination nanoemulsions.	26
Table 3. Hydrodynamic Diameter and Polydispersity Index of Nanoemulsions.....	28
Table 4. Zeta Potential of Nanoemulsions..	29
Table 5. Docetaxel HPLC Loading Efficiency.	30
Table 6. Average IC50 Values for Nanoemulsions Tested on SKOV-3 cells.....	31

Acknowledgements

Our team would like to recognize those who were involved in making this project a possibility and who supported us throughout the duration of the project. We would like to thank the following people from our sponsor, NemuCore Medical Innovations, for providing us with direction, supplies, lab equipment, and their expertise throughout the year: Dr. Tim Coleman, *President and CEO*; Dr. Nirav Patel, *Principal Scientist*; and Dr. Alex Piroyan, *Principal Scientist*. We would also like to thank our project advisors Dr. Mike Buckholt and Dr. Jill Rulfs (Worcester Polytechnic Institute) for their guidance, support, and encouragement throughout the year.

Authorship

Both team members spent equal amounts of time working in the lab as well as on the report for this project.

Abstract

Ovarian cancer, when treated with platinum and taxanes, is frequently detected in later stages and often develops multi-drug resistant properties. Therefore, chemotherapy regimens can become ineffective, leaving clinicians with less efficacious therapies. Our hypothesis is that a nanotherapy approach, utilizing nanoemulsions (NE) to deliver a combination of drugs with synergistic mechanisms of action, will likely reduce the spread of ovarian cancer and deliver the combination with reduced systemic toxicity. Results suggest that combination NEs can be manufactured and show some promise to kill ovarian cancer cells more efficiently.

Background

Introduction

Despite substantial improvements in ovarian cancer treatments, optimizing drug efficacy and minimizing drug toxicity continues to be an important concern. Initially, most ovarian cancers are sensitive to chemotherapy, but with continued use can result in multi-drug resistance of cancers. In order to overcome multi-drug resistance while enhancing potency, a novel way of delivering therapies is needed.

Part 1: Ovarian cancer

Disease Statistics

Ovarian cancer accounts for 3% of cancer in women. (American Cancer Society, 2014). It was projected that for 2014, 21,980 women would receive a new diagnosis of ovarian cancer and 14,270 would die from the disease (American Cancer Society, 2014). In the course of a woman's lifetime, the risk of being diagnosed with ovarian cancer is about 1 in 73, although it mainly develops in older white women, particularly 60 years or older (American Cancer Society, 2014). In the past, ovarian cancer has tended to remain clinically silent until the disease had reached an advanced stage that predominantly remained intraperitoneal throughout its course (Longo & Young, 1981). The percent of the population affected by ovarian cancer is relatively low and the detection of the disease is difficult, the 5-year survival rate is extremely low (Parkin, 2011), thus making it a large unmet clinical need.

Types of Ovarian Cancer

Far too often, ovarian cancer is detected in its late stages, making it extremely difficult to treat. Often, the disease is identified clinically as tumors that grow in the ovaries. These tumors can either be benign, borderline, low malignant potential (LMP), or

malignant (Johns Hopkins Pathology, 2001). Benign tumors will not metastasize; however, malignant cells tend to metastasize in two ways. First malignant cells can metastasize by directly migrating to other organs in the pelvic or abdominal region (Ovarian Cancer National Alliance, 2014). The second and less common way for malignant tumors to spread throughout the body is through the bloodstream or lymph nodes (Ovarian Cancer National Alliance, 2014). Part of the difficulty of detecting ovarian cancer early is due to the unknown initial causes. Some theories that may explain the cause of ovarian cancer include genetic errors due to “wear and tear” of the monthly release of the egg or increased hormone levels before and during ovulation that can stimulate the growth of abnormal cells (Ovarian Cancer National Alliance, 2014). The ovaries, which are involved in both the reproductive and endocrine body systems, are small organs that are responsible for maintaining the health of the female reproductive system.

The ovaries are very complex. Because of their complexity, there are over 30 different types of ovarian cancer, all affecting and localizing different parts of the ovaries (Ovarian cancer National Alliance, 2014). The most common forms of ovarian cancer can be found in three distinct cell types: epithelium, germ cells, or stromal cells. The first of these is the ovarian surface epithelium. Surface epithelium cells are a modified mesothelium that can give rise to human ovarian carcinomas. The surface epithelium cells can quite often assume atypical morphologies, known as abnormal cells, which make it extremely difficult to identify normal epithelial cells (Auersperg et al. 1994). Surface epithelial tumors tend to account for about 60% of all ovarian cancer neoplasms (Johns Hopkins Pathology, 2001). Second, ovarian cancer tumors can be found in germ cells. These cells are totipotent progenitors that are destined to become female germ cells, or oocytes (Bukovsky et al.

2006). Germ cell neoplasms make up the second largest amount of ovarian neoplasms at about 20% (Johns Hopkins Pathology, 2001). The third cell type in which ovarian cancer tumors can be found are stromal cells. Stromal cells are spindle-shaped morphologically, similar to fibroblasts, organized into a whorled texture (King, 2013). The highly vascular tissues comprised of stromal cells account for about 10% of all ovarian neoplasms (Johns Hopkins Pathology, 2001).

Stages

Ovarian cancer severity is clearly defined in four stages: Stage I (A, B, and C), Stage II (A, B, and C), Stage III (A, B, and C), and Stage IV (National Ovarian Cancer Coalition, 2014). Each stage designates the spread or progression of the disease. The intensity ranges from Stage I, limiting the growth of cancer to the ovary or ovaries, to Stage IV in which the ovarian cancer has spread out of the abdomen towards the liver (Texas Oncology, 2014). Figure 1 shows the intensity of cancer in each of the four stages. The smaller green dots represent the cancer, and as the stages increase, the amount of cancer as well as the surface area covered by cancer increases.

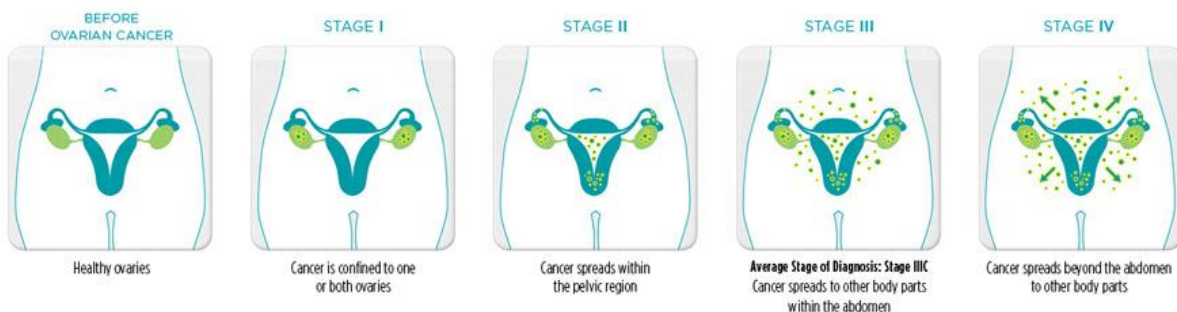


Figure 1. The stages of ovarian cancer. From left to right, the stages of ovarian cancer are shown starting with no cancer and ending with Stage IV ovarian cancer (Cannistra, 1993).

Existing Treatments

The treatment of ovarian cancer continues to be difficult today due to difficulty in diagnosing the disease until it has reached an advanced stage. However, the regimen of drug and delivery method has changed to reduce side effects and improve tumor reduction. In the 1980s, scientist believed the primary forms of treating the disease were either surgery to remove tumors or radiation therapy (Longo & Young, 1981). Other typical treatment forms were chemotherapy using single agents as well as combination therapies. Single agents included melphalan, 5-fluorouracil, and hexamethylmelamine (Long & Young, 1981). Melphalan is a nitrogen mustard alkylating agents that attach an alkyl group to DNA to induce apoptosis; fluorocil works to induce apoptosis by inhibiting cell synthases; and hexamethylmelamine also works to induce apoptosis through alkylating agents (Long & Young, 1981). Chemotherapy using combined therapies would consist of a strict regimen of particular schedules and concentrations of drugs formulated for intravenous infusion into the body.

The treatments that show efficacy in ovarian cancer therapy have greatly advanced in the last 30 years. Generally, ovarian cancer is a chemosensitive disease and the many chemotherapies have been tested to improve progression free survival (Ozols, 2006). Chemotherapy can be administered using either an intravenous (IV) or intraperitoneal (IP) delivery method. IV methods are administered through the vein whereas IP methods are delivered directly into the peritoneal cavity (Ozols, 2006). The IP method is able to deliver more drug directly to tumor sites than IV administration (Ozols, 2006). Since the late 90s, ovarian cancer has been most commonly treated with cytoreductive surgery followed by combination chemotherapy (Eisenkop et al., 1998). The cytoreductive surgery removes as

much of the tumor as possible. Naturally, cells will remain behind, leaving the ability for the tumor to regrow and possibly spread. In order to keep the ovarian cancer progression free for as long as possible, a combination chemotherapy method is used. Usually, the combination is based on a platinum compound and a taxane. The most common platinum based compounds used are carboplatin and cisplatin, while the standard taxanes used are paclitaxel or docetaxel (American Cancer Society, 2014). Platinum is mediated by an active species that interacts with DNA, RNA, and protein. The platinum-induced DNA damage causes the cell to undergo apoptosis (Agarwal, 2003). Taxanes act by binding to β -tubulin, which stabilizes the microtubule and induces apoptosis because the cell cannot divide (Agarwal, 2003). A common regimen of chemotherapy, particularly for epithelial ovarian cancer, consists of three to six cycles. The platinum-taxane combination is administered IV every three to four weeks (American Cancer Society, 2014). If the disease is in its later stages, III or IV, the chemotherapy regimen is usually administered IP. It is very well known that the method of cytoreductive surgery followed by strict chemotherapy has improved 5-year survival in patients diagnosed with ovarian cancer (Vasey et al., 2004).

Part 2: Cell Death

Programmed cell death is an intrinsic mechanism for cell death that is regulated by the cell (Edinger, 2004). In order to destroy tumor cells, cell death has to be initiated in the cells. Three known types of cell death include apoptosis, necrosis, and autophagy. Figure 2 illustrates the differences among the different types of cell deaths. Autophagic cell death (2b) shows the cell eating itself; apoptotic cell death (2c) shows the cell intrinsically destroying itself; and necrotic cell death (2d) shows catastrophic cell death.

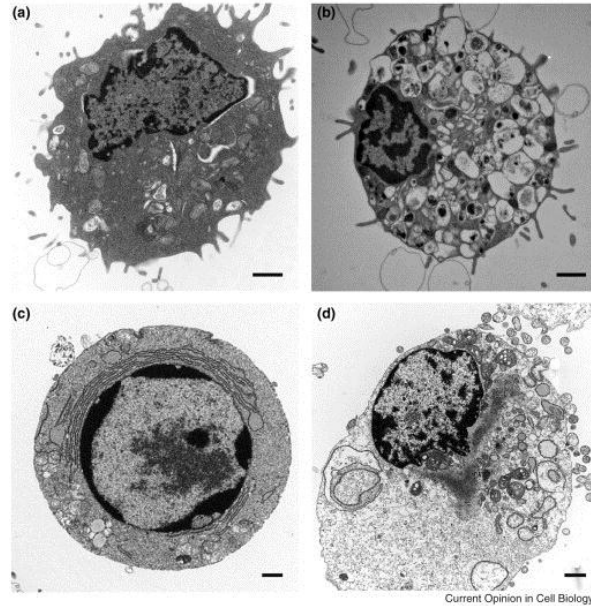


Figure 2.The types of cell death. **a.** Normal cell. **b.** Autophagic cell death. **c.** Apoptotic cell death. **d.** Necrotic cell death. (Edinger, 2004).

Apoptosis

Apoptosis is a programmed cell death that requires ATP and cellular signaling in order to initiate cell suicide. In order for apoptotic death to occur, the cell must undergo nuclear condensation and fragmentation as well as cleave chromosomal DNA into internucleosomal fragments (Edinger, 2004). The cell morphs into apoptotic bodies when a ligand attaches to a death receptor or when the mitochondria releases apoptotic mediators and activates cysteine proteases (Edinger, 2004). After apoptotic cell suicide, phagocytes remove apoptotic bodies, thus eliminating inflammation from the site of cell death (Edinger, 2004).

Necrosis

Necrosis is a passive form of cell death that is the result of a bioenergetic catastrophe. Cellular accidents such as toxins or physical damage initiate ATP depletion to a level incompatible with cell survival, thus causing the catastrophe to occur (Edinger, 2004). In necrosis, a vacuole encapsulates the cytoplasm and breaks down the plasma

membrane; as a result, inflammation surrounds the dying cell and cellular contents are released (Edinger, 2004).

Autophagy

Autophagy is a passive form of cell death in which the cell digests itself as a suicide strategy. In autophagy, cells switch to a catabolic program in which cellular constituents are degraded for energy production as a survival mechanism during periods of nutrient stress (Edinger, 2004). Cells utilize a double membrane vesicle in the cytosol to encapsulate the organelles and cytoplasm, and then the vesicle fuses with a lysosome in order to degrade and recycle the cell contents (Edinger, 2004). Autophagy is unlike apoptosis and necrosis in that it does not use up ATP destroying the cell.

Part 3: Emerging, Innovative Cancer Therapies

Cytotoxics

Docetaxel

Certain chemotherapies, such as docetaxel, a potent anticancer drug used to treat various types of cancers, is being used in safer more effective ways. Docetaxel is typically given as a free drug that has been formulated for IV infusion, and it inhibits cell growth by binding to microtubules, stabilizing the microtubules, and preventing their depolymerization (Feng, 2011). More specifically, docetaxel binds to the β -tubulin, stabilizes the cell's microtubule, prevents cell depolymerization, and causes cell cycle arrest (Huynh, 2009). However, ovarian cancer cells are susceptible to taxane-resistance. Docetaxel resistance may occur because of an overexpression of the p-glycoprotein gene on a cell or because of mutations on the β -tubulin (Bush, 2013).

Docetaxel has been chosen over other taxanes such as paclitaxel because docetaxel has a 19-fold greater potency and a 3-fold lower efflux rate than paclitaxel (Feng, Mumper,

2013). Docetaxel, shown in Figure 3a, differs structurally from paclitaxel, shown in in Figure 3b, because it has a hydroxyl group on the 10-position, and it has $-OC(CH_3)_3$ moiety at the 3' position (Feng, 2013). Docetaxel is also 10-fold more soluble in water than paclitaxel, making it easier to dissolve and encompass into various chemotherapeutic treatments.

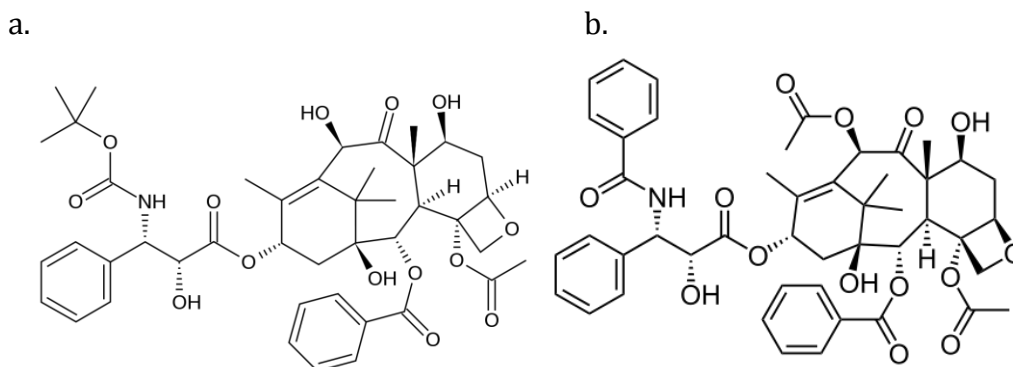


Figure 3. Docetaxel. **a.** Docetaxel has a hydroxyl functional group on carbon 10 and a tert-butyl carbamate ester on the phenylpropionate side chain. **b.** Paclitaxel has an acetate ester on carbon 10 and a tert-butyl carbamate ester on the benzyl amide side chain.

Ceramide

Ceramide is a waxy lipid molecule composed of sphingosine and a fatty acid, as shown in Figure 4. Ceramide is involved in various types of cell signaling that may regulate apoptosis, differentiation, or proliferation. Ceramide uses cellular signaling to initiate programmed cell death in cancer cells; ceramide sends signals to cells to induce the tumor necrosis factor (TNF), which in turn reduces cellular nutrients as well as causes DNA fragmentation (Obeid, 1993). Ceramide, specifically C6-ceramide, works well with the anti-tumor effects of taxols because it sensitizes taxane induced cancer cell death (Ji, 2010). Decreasing cellular ceramide levels increase tumor growth and metastasis (Guenther, 2008). Cancer cells have the ability to suppress autophagy and facilitate metabolic quiescence – state of reversible cell cycle arrest (Guenther, 2008). Therefore,

incorporating ceramide with docetaxel treatment could overcome drug resistance and sensitize the cells to docetaxel.

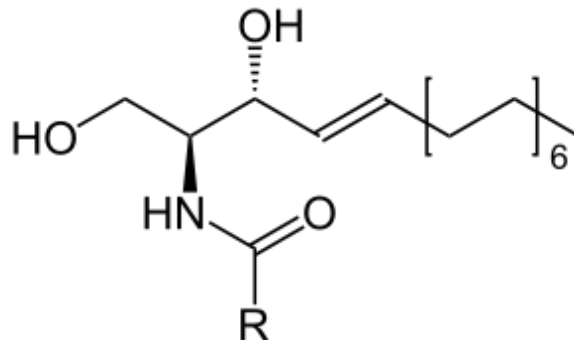


Figure 4. Ceramide. Ceramide consists of a long sphingosine linked to a fatty acid.

Kinase Inhibitors

Plasticity of the Kinome

Protein kinases are enzymes that are responsible for much of cell signaling. The enzymes are responsible for mitotic progression and spindle assembly checkpoint function (SAC silencing) (Bush, 2013). The body contains about 518 different kinases, which are grouped into families by the homology of their catalytic domain, making up the kinome (Midland, 2012). The kinome is unique in that it is capable of rapidly responding and remodeling to selective pressures (Graves, 2013). The plasticity of the kinome can interfere with various chemotherapeutic techniques because the kinases develop resistance to kinase inhibitors (Barouch-Bentov, R., 2011).

Kinase inhibitor resistance may occur if there is protein kinase overexpression or expression of inhibitor-resistant mutation; alterations in drug import/export that affect intracellular drug levels; clonal evolution as the result of additional genetic abnormalities; or upregulation of alternative signaling pathways (Cooper, 2013). Therefore, it is important to introduce kinase-inhibiting chemotherapeutics that can target multiple kinases in order to reduce resiliency (Midland, 2012).

Staurosporine

One of the kinase inhibitor drugs, staurosporine, has been proven to inhibit cyclin-dependent kinases (CDKs), one of the kinase families, and activate apoptosis (Senderowicz, 2002). Staurosporine works as a competitive inhibitor that has a strong affinity towards the ATP binding sites of *multiple* kinases, such as CDKs; therefore, it prevents ATP from binding to the kinase and activates apoptosis. Specifically, UCN-01, a clinically relevant staurosporine derivative, competes with ATP to inhibit CDKs, thus inhibiting calcium-dependent isozymes (Senderowicz, A. 2002). UCN-01 inhibits phosphorylation of Cdc25c by kinase CDK1, and as a result, the cell undergoes cycle arrest and apoptosis is activated. (Senderowicz, 2002). The ability of staurosporine to inhibit many different types of kinases may allow for greater kinetic effects on cell death

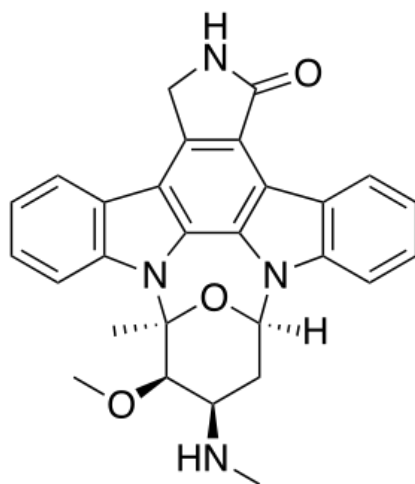


Figure 5. Staurosporine. Staurosporine contains a sugar molecule and a planar heterocyclic group.

Nanomedicines

Nanotherapy has been used as a drug delivery system to minimize drug toxicity as well as enhance drug permeability to cancerous tissues. Nanomedicine including micelles, liposomes, nanoemulsions, solid lipid nanoparticles, nanocapsules and polymeric nanoparticles have the ability to increase drug pharmacokinetics (Feng, 2011).

Nanomedicines are capable of longer circulation of delivery vehicles as well as longer retention of anticancer agents (Feng, 2011). In addition, nanoparticle surfaces can be modified with ligands which are able to target specific receptors in the tumor and increase drug uptake.

Nanoemulsions are nanomedicine platforms that have a lipid core with an aqueous surrounding, stabilized by an amphiphilic phospholipid monolayer (Figure 6a). The lipid core consists of flaxseed oil that is made up of 57% Omega-3 and 17% Omega-6 fats. The oil core has the ability to hold highly toxic, non-water-soluble drugs and protects the drugs from degradative factors both in the blood and in tumor cells. The aqueous solution that coats the oil core consists of dissolved egg lecithin, PEG₂₀₀₀DSPE, and glycerol water, distilled water with a small amount of glycerol in it. The polyethylene glycol (PEG), shown in Figure 6b, that coats the oil core prevents clearance by the mononuclear phagocyte system. Cancer specific targeting ligands can be attached to the PEG on the surface of the molecule, thus directing the NEs through leaky vasculature of the tumor and specifically to desired cancerous tissues. The desirable formulation characteristics of nanoemulsions include a monodisperse particle size of less than 200nm, apparent drug entrapment efficiency, and a negative surface charge of repulsion/attraction between particles known as a negative zeta potential (Feng, 2011).

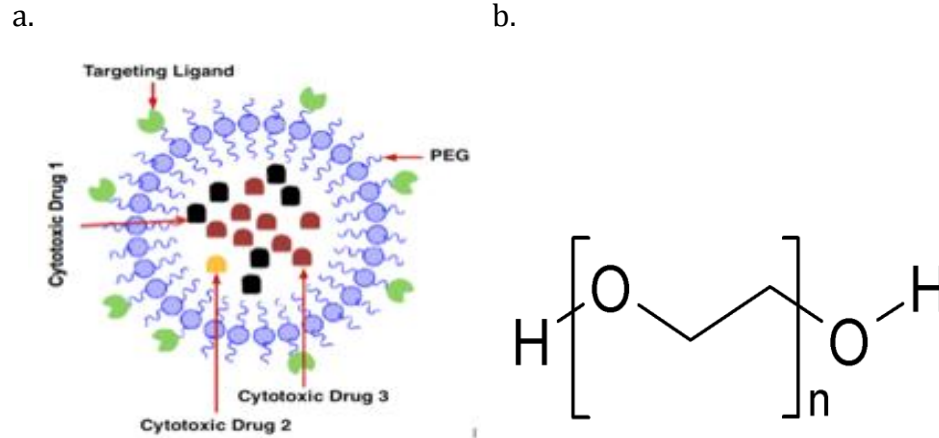


Figure 6. Diagram of Generic Nanoparticle. **a. Nanoemulsion.** The combined aqueous and oil phase contains the cytotoxic drugs on the inside and the targeting ligand on the outside. **b. PEG.** The PEG that is on the outside of Figure 6a that the targeting ligand attaches to.

Folate Targeting

Surface Foliates

Folate receptors (FR) can be found on the surfaces of certain epithelial cells throughout the body. In particular, FR α is a receptor coded by the folate receptor 1 gene and binds to folic acid with high affinity. FR α is a protein overexpressed and unregulated in ovarian cancer due to a high dependency on folate metabolism, yet is often absent from normal healthy tissue (Wen *et al*, 2015). FR α transports folate through membranes by receptor-mediated endocytosis (Wen *et al*, 2015). Essentially, drugs targeted with folate conjugates have become a novel mechanism for delivering nanoparticles to tumor sites because of their absorption through the plasma membrane. This process is known as folate targeting.

Research has been applied to create folic-acid (FA) conjugates and link them to drugs. Specifically, FA can be attached polyethylene glycol-phosphatidylethanolamine (PEG-PE) and used as a targeting ligand (Sawant & Torchilin, 2010). This allows a targeted therapy that includes a FA-PEG-PE combination to exploit the cytotoxic effects of the

encapsulated drug while simultaneously lowering the collateral damage in healthy tissue (Dongen *et al*, 2014).

In fact, a nanoemulsion is a useful nanotherapy platform that can be targeted with folate. As explained earlier, a nanoemulsion is comprised of an oil core with lipid and PEG-PE outer layer. The combination of different length PEG in the outer layer gives folate a significant freedom of rotation. There are many different forms of PEG, ranging from 500 Daltons to 60,000 Daltons. The greater length of PEG is proportional to a greater freedom of rotation of folate, however if PEG is too large, it may override the hydrophobicity of the combined lipid and pull itself out of the nanoemulsion. Because of therapies like nanoemulsions, there are now many opportunities to readily target common chemotherapies by intravenously injecting folate-targeted nanotherapies which can bypass p-glycoprotein, which naturally pumps hydrophobic drugs out of the tumor cell. Theoretically, using folate targeting as part of the delivery method in a nanoemulsion would deliver more drug to the tumor than previous free drug chemotherapy methods.

Avidity and Affinity

Folate targeted drugs have an obvious affinity for folate receptors found on tumor cells. This affinity can be measured by the dissociation constant (K_d). Typically, the K_d of folic acid when binding to folate receptors is about 10^{-9} M. In the previous section “Surface Folates”, monovalent folate-targeted drugs were said to increase the amount of drug that reaches the tumor. However, it has been seen that dissociation has a direct correlation with the average valency of FA conjugates. Therefore, as the average valency of FA conjugates to $FR\alpha$ is increased, the dissociation of the folate-targeted drug has been seen to decrease, thus increasing the affinity of folate targeted nanotherapies (Dongen *et al*, 2014).

Swanson *et al* used gadolinium-loaded dendrimer nanoparticles targeted with folate to show the affinity that folate-targeted nanoparticles have for the overexpressed FR α cancer cells. Gadolinium (Gd) is detected in quantity through MRI, as it is an imaging agent. The study conducted by Swanson *et al* showed enhanced gadolinium accumulation in KB human tumors over 24 hours for targeted dendrimers when compared to non-targeted dendrimers. This further supported the idea that targeting a drug with FA increases the affinity and avidity of the therapy.

Part 4: Hypothesis and Specific Aims

It is our hypothesis that the combination of docetaxel, ceramide, and staurosporine encapsulated in a folate targeted nanoemulsion will deliver a safer and more effective treatment to ovarian cancer. A problem that occurs in trying to treat ovarian cancer is the speed at which multi drug resistance develops. The current delivery methods damage the body while not always treating the tumor(s). The encapsulation technique used to engineer nanoemulsions prevents this effect by protecting the enclosed drugs from metabolic deactivation and nonspecific drug interactions. If the nanoemulsions can remain stable by exhibiting no significant changes in size, zeta potential, and drug payload, then the nanomedicines can be successful treatment options.

Multidrug resistance can be combated through the use of three different drugs in combination. The combination of drugs targets a variety of pathways that create a superior apoptotic effect. At the same time, the nanoemulsion controls the delivery of a highly toxic payload because of the folate targeting and encapsulation of the drugs. The optimal combinational therapies at minimal toxicity levels are determined through IC₅₀ testing.

Materials and Methods

General Manufacturing Nanomedicines

Nanoemulsions consist of an aqueous phase as well as an oil phase. Hydrophobic active pharmaceutical ingredients (APIs) were loaded into the oil phase of each nanoemulsion. The hydrophobic APIs used in this project included docetaxel (DTX), ceramide (CER), and staurosporine (STP). A total of 5 nanoemulsions were made by loading the following combinations of APIs into oil phases: docetaxel; docetaxel and ceramide; docetaxel, ceramide, and staurosporine; staurosporine; and staurosporine and ceramide. The APIs were loaded in a concentration of 50:10:1 ceramide: docetaxel: staurosporine. Polyethylene Glycol (PEG), the pegylating agent, and Egg Lecithin, an emulsifying agent, were added to the aqueous phase with glycerol, an agent necessary for maintaining isotonicity in nanoemulsions. The aqueous phase also contained folate-targeting ligands conferring specificity to the NEs to receptors, often overexpressed on ovarian cancer cells. The aqueous phase was kept on a stir plate until all ingredients were dissolved.

Once the phases were prepared, the two were combined and vortexed to create an emulsion. The combined emulsion was processed through an LV1 Microfluidizer for 10 cycles at 25,000 PSI. The final concentration of docetaxel drug was determined using an HPLC instrument, and the final concentration of the drug usually ranged from 1mM to 2mM. The size and surface charge of the nanoparticles were read on the ZetaSizer. The sizes ranged from 130 – 160nm, and the zeta potential ranged from -40 to -60mV. Nanoemulsions were stored at 4°C.

HPLC Method of Detecting DTX

The concentration of docetaxel loaded into each of the nanoemulsions was determined via High Performance Liquid Chromatography (HPLC). The Water HPLC contained a Malvern 1525 Binary HPLC Pump with a Thermo Scientific Hypersil gold column (C18 5 μ M, Size – 150x4.6 mm) and a Malvern 2487 Dual Absorbance Detector UV detector. The flow rate was always set to 1 ml/min. Standard curves consisting of 75 μ g/ml, 50 μ g/ml, 40 μ g/ml, 25 μ g/ml, 12 μ g/ml, and 6.25 μ g/ml of docetaxel in acetonitrile (ACN) were established at the beginning of each assay. In between samples, the HPLC system was washed with 100% ACN.

The mobile phase used to quantify docetaxel was comprised of 60% ACN and 40% water. The UV detector was set to 270 nm. The retention time of docetaxel was approximately 2-3 minutes.

The remaining drugs that were used in this study – ceramide and staurosporine – were not analyzed using the HPLC. The amount of staurosporine loaded into nanoemulsions was too small to detect, and a method to determine the amount of ceramide in the nanoemulsion had not been determined.

Quantification of APIs in Nanomedicines

Nanoparticle samples were diluted 1,000 fold in ACN, vortexed for 2 minutes, and then spun down in a centrifuge for 10 minutes at 10,000rpm. Supernatant was then analyzed on HPLC using the method above.

Cell Lines

The human ovarian cancer cell line, SKOV-3 was obtained from the ATCC (Manassas, VA). SKOV-3 cells were continuously cultured in RPM1 1640 media with L-glutamine

containing 10% fetal bovine serum and 1% penicillin/streptomycin, in a humidified incubator at 37°C with 5% CO₂. All cell culture media as well as sterile equipment used was purchased from Fisher Scientific.

Cytotoxicity Assay

Cell viability and 50% inhibitory concentration (IC₅₀) values were generated using the 3-(4,5-dimethylthiazol-2-yl)-2,5-diphenyltetrazolium bromide (MTT) assay. SKOV-3 cells were seeded into 96-well plates at a density of 3 X 10³ cells/well in normal growth media and incubated 24 hours incubation for proper attachment and cell cycle synchronization. Following incubation, media was removed and replaced with proper dosing of drug containing media. Table 1 shows the plate layout for cells dosed with just docetaxel. The IC₅₀ for cells plated with just docetaxel or docetaxel, ceramide loaded nanoemulsions were higher than other nanoemulsions thus the different concentrations in the plate layout. The plates of cells dosed with staurosporine and combinational therapies were dosed according to the plate layout in Table 2. Staurosporine was effective at lesser concentrations, so the doses were 10-fold less in Table 2.

Table 1. The plate layout for cells dose with docetaxel nanoemulsions. This plate layout was used for nanoemulsions loaded with docetaxel only or docetaxel and ceramide.

	1	2	3	4	5	6	7	8	9	10	11	12
A	PEI	Untreated	0.00001 μM	0.0001 μM	0.001 μM	0.01 μM	0.1 μM	1 μM	10 μM	100 μM	Untreated	Untreated
B	PEI	Untreated	0.00001 μM	0.0001 μM	0.001 μM	0.01 μM	0.1 μM	1 μM	10 μM	100 μM	Untreated	Untreated
C	PEI	Untreated	0.00001 μM	0.0001 μM	0.001 μM	0.01 μM	0.1 μM	1 μM	10 μM	100 μM	Untreated	Untreated
D	PEI	Untreated	0.00001 μM	0.0001 μM	0.001 μM	0.01 μM	0.1 μM	1 μM	10 μM	100 μM	Untreated	Untreated
E	Blank	Untreated	0.00001 μM	0.0001 μM	0.001 μM	0.01 μM	0.1 μM	1 μM	10 μM	100 μM	Untreated	Untreated
F	Blank	Untreated	0.00001 μM	0.0001 μM	0.001 μM	0.01 μM	0.1 μM	1 μM	10 μM	100 μM	Untreated	Untreated
G	Blank	Untreated	0.00001 μM	0.0001 μM	0.001 μM	0.01 μM	0.1 μM	1 μM	10 μM	100 μM	Untreated	Untreated
H	Blank	Untreated	0.00001 μM	0.0001 μM	0.001 μM	0.01 μM	0.1 μM	1 μM	10 μM	100 μM	Untreated	Untreated

Table 2. The plate layout for cells dose with staurosporine and/or combination nanoemulsions. This plate layout was used for nanoemulsions loaded with staurosporine only; staurosporine and ceramide; or staurosporine, docetaxel, and ceramide.

	1	2	3	4	5	6	7	8	9	10	11	12
A	PEI	Untreated	0.000001 μM	0.00001 μM	0.0001 μM	0.001 μM	0.01 μM	0.1 μM	1 μM	10 μM	Untreated	Untreated
B	PEI	Untreated	0.000001 μM	0.00001 μM	0.0001 μM	0.001 μM	0.01 μM	0.1 μM	1 μM	10 μM	Untreated	Untreated
C	PEI	Untreated	0.000001 μM	0.00001 μM	0.0001 μM	0.001 μM	0.01 μM	0.1 μM	1 μM	10 μM	Untreated	Untreated
D	PEI	Untreated	0.000001 μM	0.00001 μM	0.0001 μM	0.001 μM	0.01 μM	0.1 μM	1 μM	10 μM	Untreated	Untreated
E	Blank	Untreated	0.000001 μM	0.00001 μM	0.0001 μM	0.001 μM	0.01 μM	0.1 μM	1 μM	10 μM	Untreated	Untreated
F	Blank	Untreated	0.000001 μM	0.00001 μM	0.0001 μM	0.001 μM	0.01 μM	0.1 μM	1 μM	10 μM	Untreated	Untreated
G	Blank	Untreated	0.000001 μM	0.00001 μM	0.0001 μM	0.001 μM	0.01 μM	0.1 μM	1 μM	10 μM	Untreated	Untreated
H	Blank	Untreated	0.000001 μM	0.00001 μM	0.0001 μM	0.001 μM	0.01 μM	0.1 μM	1 μM	10 μM	Untreated	Untreated

RPMI media was used as a negative control (0% cell death). Poly(ethyleneimine), was used as a positive control (100% cell death) and was prepared at a concentration of 0.25 mg/ml. Depending on the kinetics experiment, after either 24, 48, or 72 hours of incubation, the MTT assay was performed following the accepted standard protocol. The absorbance was measured at 570 nm using the plate reader. The treatment which reduced 50% of cell viability (IC₅₀) was calculated using GraphPad® Prism 5.

Results

Manufacturing and Monitoring Stability of Nanomedicines

Five different nanoemulsions were engineered throughout this project: one encapsulating docetaxel (DTX); one encapsulating docetaxel and ceramide (CER); one encapsulating docetaxel, ceramide, and staurosporine (STP); one encapsulating staurosporine; and one encapsulating staurosporine and ceramide. The nanoemulsions were engineered using Microfluidics High Pressure Homogenizer LV1. The LV1 Microfluidizer takes the crude mixture of an aqueous phase and an oil phase and puts it through tiny porous membranes at a high pressure. The LV1 Microfluidizer takes the size of the nanoemulsions down to the nano-scale and produces a homogenous colloidal suspension. After the nanoemulsions have gone through the suggested number of cycles in the LV1 Microfluidizer, the size and the zeta potential was measured on the Malvern SV90 ZetaSizer, a machine that uses Dynamic Light Scattering to calculate the average size and distribution of the nanoemulsions.

The stability of the nanoemulsions was monitored to ensure the reliability of the molecules for an extended period of 28 days. **Table 3** shows the hydrodynamic diameter and polydispersity index (PDI) for each of the five nanoemulsions measured every 7 days for 28 days, starting with the day the nanoemulsion was synthesized (day 0). The PDI is a numeric representation of the dispersion of sizes, therefore the higher the PDI, the more variety in particle size. Table 3 shows that there was little variability in the hydrodynamic diameters for each of the nanoemulsions, and there was no significant variance in PDI. The hydrodynamic diameter is expected to be less than 180nm to ensure safety when injected into the blood. A nanoparticle greater than 180nm could be too large and cause an

embolism. Each of the five nanoemulsions synthesized had hydrophobic diameters less than 180nm that remained stable over the 28 days.

Table 3. Hydrodynamic Diameter and Polydispersity Index of Nanoemulsions. Each nanoemulsion size distribution was determined every 7 days for 28 days using a ZetaSizer. DTX, CER and DTX, CER, and STP nanoemulsions do not have data for day 28 because the nanoemulsion was used up by this time in cytotoxicity assays.

NE	Hydrodynamic Diameter (nm)					Polydispersity Index (\pm)				
	Day					Day				
	0	7	14	21	28	0	7	14	21	28
DTX	139.2	138.8	136.7	136.7	141.7	0.021	0.050	0.035	0.074	0.073
DTX, CER	132.4	132.2	133.4	130.5	N/A	0.030	0.037	0.043	0.002	N/A
DTX, CER, STP	129.4	131.4	125.9	121.3	N/A	0.051	0.037	0.063	0.071	N/A
STP	150.7	164.0	161.0	154.0	158.5	0.039	0.079	0.059	0.038	0.047
STP, CER	128.1	134.6	137.5	135.4	132.1	0.081	0.089	0.105	0.096	0.094

The ZetaSizer was also used to measure the zeta potential of each nanoemulsion. The nanoemulsions are expected to be slightly negative so that upon entry to the body, the concentrations of cations such as sodium and potassium in the body do not make the particles too positive, which could cause an embolism. Table 4 shows the zeta potentials obtained for each nanoemulsion measured every 7 days for a period of 28 days. The zeta potentials stayed stable in a range of -30 to -50mV, which is what is expected for nanoemulsion charge. The standard deviations (SD) are included in the table.

Table 4. Zeta Potential of Nanoemulsions. Each nanoemulsion zeta potential was determined every 7 days for 28 days using a ZetaSizer. DTX, CER and DTX, CER, and STP nanoemulsions do not have data for day 28 because the nanoemulsion was used up by this time in cytotoxicity assays.

NE	Zeta Potential \pm SD (mV)				
	Day				
	0	7	14	21	28
DTX	-48.7 \pm 10.4	-45.8 \pm 9.02	-51.5 \pm 5.39	-44.5 \pm 6.34	-49.3 \pm 11
DTX, CER	-46.5 \pm 8.51	-47.7 \pm 9.72	-50.7 \pm 10.6	-51.6 \pm 9.27	N/A
DTX, CER, STP	-42.5 \pm 8.16	-43.1 \pm 9.47	-46.9 \pm 8.79	-48.2 \pm 12.2	N/A
STP	-43.0 \pm 9.75	-43.2 \pm 10.2	-46.0 \pm 10.6	-48.4 \pm 12.0	-42.1 \pm 7.37
STP, CER	-48.2 \pm 10.2	-41.2 \pm 10.7	-39.7 \pm 11.4	-43.1 \pm 9.63	-41.0 \pm 7.74

HPLC Detection of DTX

Each nanoemulsion containing docetaxel was assayed to confirm the concentration of the docetaxel loaded into the nanoemulsion using a Waters HPLC Pump. The mobile phase of the HPLC was set to 30% Acetonitrile and 20% distilled water, with a flow rate of 1 mL/min. The HPLC mobile phase was only set to a total of 50% to prevent clogging in the column. A standard curve was constructed with docetaxel dissolved in Acetonitrile. The nanoparticles were diluted 1:1000 in Acetonitrile and vortexed for approximately 2 min in order to lyse the particles and free the docetaxel. The supernatant from the dilution was put through the HPLC to measure drug concentration.

Table 5 shows the milligram of docetaxel loaded into each nanoemulsion, the amount of docetaxel detected in the HPLC assay (in milligrams per milliliter), the amount of docetaxel detected in the HPLC assay (in micrograms per milliliter), and the percentage of loading efficiency for each nanoemulsion. Molarity was used to determine treatment

concentrations for the plates. The docetaxel nanoemulsion had an 80.25% loading efficiency, indicating that of the 2mg/ml put into the nanoemulsion, 80.25% of the docetaxel actually loaded into the nanoemulsion. The docetaxel, ceramide nanoemulsion had a 106.3% loading efficiency, meaning that of the 0.8 mg/ml put into the nanoemulsion, 106.3% actually loaded into the emulsion. Having a loading efficiency over 100% is plausible because the sample we took to assay may have contained slightly more docetaxel than another sample in the emulsion, suggesting that the concentration may not have been completely uniform. Lastly, our docetaxel, ceramide, and staurosporine nanoemulsion had an 83.13% loading efficiency.

Table 5. Docetaxel HPLC Loading Efficiency. Each nanoemulsion that contained docetaxel was run through HPLC to determine docetaxel loading efficiency.

NE	DTX Concentration Loaded (mg/ml)	NE DTX Concentration (mg/ml)	NE DTX Concentration (mM)	% Loading Efficiency
DTX	2	1.605	1.987	80.25
DTX, CER	0.8	0.835	1.034	106.3
DTX, CER, STP	0.8	0.665	0.823	83.13

The staurosporine and staurosporine, ceramide nanoemulsions were not assayed using the HPLC because the small amount of staurosporine in the nanoemulsions would be nearly impossible to detect.

Cytotoxicity Assays

Each of the five nanoemulsions were tested for cytotoxicity on an SKOV-3 cell line. The kinetics of the mechanism of the drug were tested at 24, 48, and 72 hours. Each nanoemulsion was tested on four 96-well plates containing SKOV-3 cells and were administered according to the plate layouts seen in Tables 1 and 2. Cytotoxicity data was collected for 24, 48, and 72 hours for each nanoemulsion with the exception of the docetaxel nanoemulsion. The 48 hour plates were infected with fungus and thus did not produce any conclusive or reportable data resulting in not reported data (N.D.). Both the staurosporine and staurosporine-ceramide nanoemulsions showed inconclusive data that cannot be reported. In the cytotoxicity assay, values are presented in both constrained and non-constrained cell viability percentages. Due to the lack of cell death in both the staurosporine and staurosporine-ceramide nanoemulsions, the constrained and non-constrained cytotoxicity data was extremely inconsistent and can therefore not be reported. The resulting reportable IC₅₀ values for the docetaxel, docetaxel-ceramide, and docetaxel-ceramide-staurosporine nanoemulsions can be seen in Table 6.

Table 6. Average IC₅₀ Values for Nanoemulsions Tested on SKOV-3 cells. Each nanoemulsion was tested on four 96-well plates of SKOV-3 cells.

NE	IC ₅₀ (Average)		
	24 hour (nM)	48 hour (nM)	72 hour (nM)
DTX NE	>100 μ M	N.D.	4.0085
DTX, CER	>100 μ M	66.6785	1.809
DTX, CER, STP	>100 μ M	91.706	3.558

Based on these results, there was not an observable or significant decrease in IC_{50} values with the addition of any drug into a nanoemulsion. Although both the DTX-CER, and DTX-CER-STP nanoemulsions showed lower IC_{50} values than the DTX nanoemulsion alone, there is no conclusive data supporting the hypothesis predicting a triple or double combination nanoemulsion with this specific ratio of drugs leads to higher cytotoxicity. However, based on this data, it is seen that at 72 hours, maximum cytotoxicity is observed for each of the three FA-targeted nanoemulsions investigated.

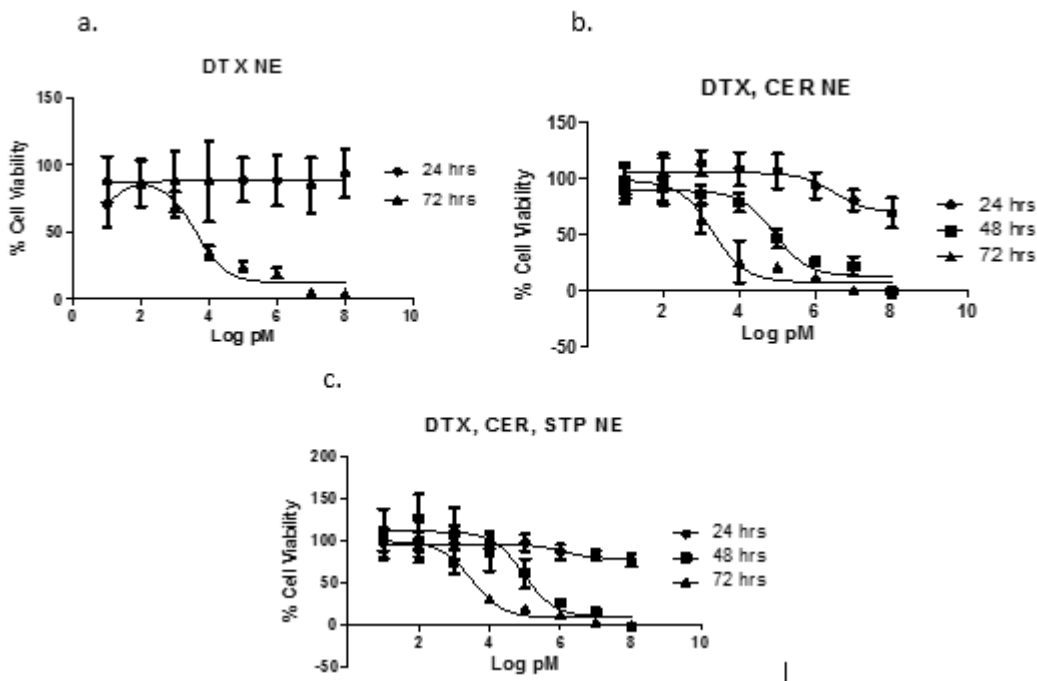


Figure 7. Cytotoxicity Results for DTX, DTX-CER, and DTX-CER-STP nanoemulsions. Maximum cytotoxicity is observed at 72 hours for all nanoemulsions. **a.** Docetaxel nanoemulsion cytotoxicity data. **b.** Docetaxel-ceramide cytotoxicity data. **c.** Docetaxel-ceramide-staurosporine cytotoxicity data.

For each of the nanoemulsions, the drug activity at 24 hours showed almost no cell death, indicating that at this time point, the drug is relatively ineffective at killing the SKOV-3 cells. For both the DTX-CER and DTX-CER-STP nanoemulsions, an improvement was seen at 48 hours, displaying higher cytotoxicity and a lower nanomolar kill. All three

nanoemulsions showed the most effective and overall maximum cytotoxicity at 72 hours. This indicates that the mechanism of action of this drug is optimum at 72 hours and effectively kills SKOV-3 cells better when compared to the mechanisms at 24 and 48 hours.

Discussion

Ovarian cancer accounts for ~3% of all cancers in women (American Cancer Society, 2014). Although the percentage may seem small, the 5-year survival rate for those suffering with ovarian cancer is very low (Parkin, 2011). Ovarian cancer is a difficult disease to detect with a clear unmet clinical need. Two of the main issues that arise with ovarian cancer are late diagnosis and multi-drug resistance. Ovarian cancer typically is not detected until it is in the third or fourth stage of the disease where tumors have metastasized to all areas of the peritoneal space (Cannistra, 1993). Treatment includes surgical removal of tumors followed by chemotherapy. Unfortunately, the p-glycoprotein in the ovarian cancer cell lines resist apoptosis and acquire multi-drug resistance by hydrophobic chemotherapeutic drug efflux or simply not allowing the drugs to enter the cell (Gottesman, 2002).

The use of targeted nanoemulsions has the ability to overcome many of the problems facing current ovarian cancer treatment. Encapsulating active pharmaceutical ingredients (API) such as docetaxel, ceramide, and staurosporine, in a nanoemulsion, and targeting the nanoemulsion towards folate-receptors, has the potential to overcome multi-drug resistance and deliver the chemotherapeutics in a less toxic way. The goal of this MQP was to synthesize and characterize 5 combination nanoemulsions, determine nanoemulsion cytotoxicity on ovarian cancer cells, and determine the kinetics of cell death of each nanoemulsion. Overall, we wanted to determine if drug combinations enhance potency.

The five nanoemulsions we synthesized maintained stability in their hydrophobic diameters and zeta potentials (see Tables 3 and 4, respectively) over the course of 28 days.

The consistency among nanoemulsions concluded that it is possible to encapsulate three chemotherapeutic drugs into a nanoemulsion and that the drugs encapsulated stay within the nanoemulsion for at least a month. The HPLC analysis further confirmed that docetaxel is successfully encapsulated into nanoemulsions.

It was previously hypothesized that the addition of staurosporine, a versatile kinase inhibitor, could alter the kinetics effects of a nanoemulsion also encapsulating docetaxel and ceramide. This triple combination drug was thought to not only alter the kinetic effects, but effectively increase cytotoxicity, essentially killing SKOV-3 cells with a lower concentration of drug. With increased cytotoxicity, less drug could be administered to a patient and decrease tumor size. However, based on the results seen in Figure 7, the combination of chemotherapeutics and pro-apoptotic factors to create a triple combination nanoemulsion does not significantly decrease the IC_{50} values as was hypothesized. However, based on the consistency of the data presented in Figure 7 and Table 6, the maximum cytotoxicity for the nanoemulsions tested was observed at 72 hours in the MTT assay. Although this specific combination and ratio of chemotherapeutics and pro-apoptotic agents did not significantly lower the IC_{50} values, it is thought that other ratios of the drugs in the nanoemulsions may still hold potential to achieve improved cytotoxicity, which remains to be tested.

The aim of this study was to develop and test a novel therapy for the treatment of multidrug resistant ovarian cancer. The results discussed in this paper provide a foundation for further experimentation and development of the therapy. The next step will include extensive *in vivo* studies in order to properly conclude the effectiveness, toxicity,

and specificity of the nanoemulsions. Further studies may include testing the staurosporine activity, adjusting the combination ratio for the cytotoxic drugs, utilizing different ovarian cancer cell lines, and testing the effectiveness of overcoming the multidrug resistance. For example, further experimentation could include trying to recover any cells that had received treatment in the MTT assays followed by trying to “re-kill” the recovered cells. Further experimentation may also include testing the media from the cells that received treatment in the MTT assays for any drug showing effluxion from the cells or for drugs that had not entered the cell in the first place. This will reveal the effects the drugs had on the cells such as any drug resistance or drug impermeability.

References

- Agarwal, R., & Kaye, S. B. (2003). Ovarian cancer: strategies for overcoming resistance to chemotherapy. *Nature Reviews Cancer*, 3(7), 502 - 516.
- Auersperg N., Maines-Bandiera SL., Dyck HG., Kruk PA. (1994). Characterization of cultured human ovarian surface epithelial cells: phenotypic plasticity and premalignant changes. *Laboratory investigation; a journal of technical methods and pathology* 71(4): 510-518.
- Bandara NA., Hansen MJ., Low PS. (2014). Effect of Receptor Occupancy on Folate Receptor Internalization. *Molecular Pharmaceutics* 11: 1007-1013. doi: 10.1021/mp400659t.
- Barouch-Bentov, R., & Sauer, K. (2011). Mechanisms of drug resistance in kinases. *Expert Opinion on Investigational Drugs*, 153-208.
- Bukovsky A., Virant-Klun I., Svetlikova M., Willson I. (2006). Ovarian Germ Cells. *Methods in Enzymology; Adult Stem Cells*, (419): 208-258. doi: 10.1016/S0076-6879(06)19010-2.
- Bush, T. L., Payton, M., & Heller, S. (2013). AMG 900, a Small-Molecule Inhibitor of Aurora Kinases, Potentiates the Activity of Microtubule-Targeting Agents in Human Metastatic Breast Cancer Models. *Molecular Cancer Tehrapeutics*, 12, 2356-2366.
- Cannistra, S. (1993). Cancer of the Ovary. *New England Journal of Medicine*, 1550-1559.
- Cooper, M. J., Graves, L. M., Roy, S. G., Jones, L. S., Nguyen, T. A., Whittle, M. C., et al. (2013). Application of Multiplexed Kinase Inhibitor Beads to Study Kinome Adaptations in Drug-Resistant Leukemia. *PLoS ONE*, 8(6), e66755.
- Dongen MA., Silpe JE., Dougherty CA., Kanduluru AK., Choi SK., Orr BG., Low PS., Holl MM. (2014). Avidty Mechanism of Dendrimer-Folic Acid Conjugates. *Molecular Pharmaceutics* 11: 1696-1706. doi: 10.1021/mp5000967.
- Edinger, A., & Thompson, C. (2004). Death by design: Apoptosis, necrosis and autophagy. *Current Opinion in Cell Biology*, 16, 663-669.
- Esenkop SM., Friedman RL., Wang H. (1998). Complete Cytoreductive Surgery Is Feasible and Maximizes Survival in Patients with Advanced Epithelial Ovarian Cancer: A Prospective Study. *Gynecologic Oncology* 69: 103-108.
- Feng, L., Benhabbour, S. R., & Mumper, R. J. (2013). Oil-Filled Lipid Nanoparticles Containing 2'-(2-Bromohexadecanoyl)-Docetaxel for the Treatment of Breast Cancer. *Advanced Healthcare Materials*, 2(11), 1451-1457.

- Feng, L., & Mumper, R. J. (2013). A critical review of lipid-based nanoparticles for taxane delivery. *Cancer Letters*, 334(2), 157-175.
- Feng, L., Wu, H., Ma, P., Mumper, R. J., & Benhabbour, S. R. (2011). Development and optimization of oil-filled lipid nanoparticles containing docetaxel conjugates designed to control the drug release rate in vitro and in vivo.. *International Journal of Nanomedicine*, 6, 2545-2556.
- Ganta, S., et al. (2014). Formulation development of a novel targeted theranostic nanoemulsion of docetaxel to overcome multidrug resistance in ovarian cancer. *Drug Delivery*, 1-13.
- Gottesman, M. & Pastan, I. (2002). Mechanisms of drug resistance in cancer therapy. *European Journal of Pharmacology*, 17-18.
- Ji, C., Yang, B., Yang, Y., He, S., Miao, D., He, L., et al. (2010). Exogenous cell-permeable C6 ceramide sensitizes multiple cancer cell lines to Doxorubicin-induced apoptosis by promoting AMPK activation and mTORC1 inhibition. *Oncogene*, 29(50), 6557-6568.
- King, D. (2013). Ovary. Southern Illinois University School of Medicine. From <http://www.siumed.edu/~dking2/erg/ovary.htm>.
- Longo DL., Young RC. (1981). The Natural History and Treatment of Ovarian cancer. *Annual Reviews of Medicine*, 1(31): 475-490.
- Midland, A. A., Gomez, S. M., Johnson, G. L., Graves, L. M., Iii, H. S., Carey, L. A., et al. (2012). Defining the expressed breast cancer kinome. *Cell research*, 22(4), 620-623.
- Ozols RF. (2006). Systemic Therapy for Ovarian Cancer: Current Status and New Treatments. *Seminars in Oncology* 33(6): S3-S11.
- Parkin, M., & Pasini, P. (1999). Erratum: Global Cancer Statistics. *CA: A Cancer Journal for Clinicians*, 134-134.
- Senderowicz, A. M. (2002). The Cell Cycle as a Target for Cancer Therapy: Basic and Clinical Findings with the Small Molecule Inhibitors Flavopiridol and UCN-01. *The Oncologist*, 7(90003), 12-19.
- Swanson, S. D., Kukowska-Latallo, J. F., Patri, A. K., Chen, C., Ge, S., Cao, Z., ... & Baker, J. R. (2008). Targeted gadolinium-loaded dendrimer nanoparticles for tumor-specific magnetic resonance contrast enhancement. *International journal of nanomedicine*, 3(2), 201.
- Vasey PA., Jayson GC., Gordon A., Gabra H., Coleman R., Atkinson R., Parkin D., Paul J., Hay A.,

Kaye SB. (2004). Phase III Randomized Trial of Docetaxel-Carboplatin Versus Paclitaxel-Carboplatin as First-line Chemotherapy for Ovarian Carcinoma. *Journal of the National Cancer Institute* 96(22): 1682-1691. doi: 10.1093/jnci/djh323.

Vlashi E., Kelderhouse LE., Sturgis JE., Low PS. (2013). Effect of Folate-Targeted Nanoparticle Size on Their Rates of Penetration into Solid Tumors. *American Chemical Society* 7(10): 8573-8582. doi: 10.1021/nn402644g.

Wen, Y., Graybill, W. S., Previs, R. A., Hu, W., Ivan, C., Mangala, L. S., ... & Sood, A. K. (2015). Immunotherapy targeting folate receptor induces cell death associated with autophagy in ovarian cancer. *Clinical Cancer Research*, 21(2), 448-459.